

## 1 **Materials and Methods**

### 2 **Animal Study and Approval**

3 C57BL/6J mice (male, 8 weeks) were sourced from Vital River Laboratory Animal  
4 Technology (Jiaxing, China) and maintained under specific pathogen-free conditions  
5 with controlled 12-hour light/dark cycles. Animals received ad libitum access to  
6 autoclaved feed and sterile water. All experimental protocols were approved by the  
7 Center for Drug Safety Evaluation and Research of Zhejiang University and performed  
8 according to the Institutional Animal Care and Use Committee (IACUC) protocol of  
9 Zhejiang University (ethical approval: IACUC-s20-025). Following one week of  
10 acclimation, drug administration commenced. Terminal procedures involved anesthesia  
11 induction with 2% isoflurane followed by cervical dislocation for tissue collection.

12 Pral (TQ0277, TargetMol, USA) was solubilized in cyclodextrin (Aladdin, H108813)  
13 to generate stock solutions. Seven- to ten-week-old mice received daily intragastric  
14 gavage of either vehicle control (cyclodextrin) or 100 mg/kg/d Pral for 28 consecutive  
15 days.

### 16 **Histopathological and Immunohistochemical Analysis**

17 Post-euthanasia lung specimens were divided into two parts. The right part underwent  
18 snap-freezing in liquid N<sub>2</sub> for storage at -80 °C. The left lobe was immersion-fixed in  
19 4% paraformaldehyde, embedded in paraffin, and sectioned at 4 μm. Tissue sections  
20 were stained with H&E and Masson's trichrome staining per standardized protocols.  
21 Pulmonary injury quantification employed the injury-severity algorithm described by  
22 Jones et al [14].

23 For IHC, sections were incubated with anti-CREB1 (ET1601-15, HuaBio, China), with  
24 subsequent whole-slide digital scanning and analysis (HS6, Sunny Instrument Co., Ltd.,  
25 Ningbo, China).

26 Multiplex immunohistochemistry (mIHC) was performed by Hunan Aifang Biological  
27 following standardized protocols. Primary antibodies utilized included: F4/80 (29414-  
28 1-AP, Wuhan Sanying, China), S100A9 (29414-1-AP, Wuhan Sanying, China),  
29 FGFR1 (ET1612-62, HuaBio, China), OCLN (27260-1-AP, Wuhan Sanying, China),  
30 SFTPC(10774-1-AP, Wuhan Sanying, China).

### 31 **Pulmonary Function Measurement**

32 To characterize the physiological consequences of Pral on lung mechanics, we  
33 evaluated respiratory function using a flexiVent apparatus (SCIREQ, Montreal,  
34 Canada). Following the induction of deep anesthesia, mice were positioned supine and  
35 firmly stabilized for consistent data acquisition. Tracheal exposure was achieved via a  
36 midline cervical incision, allowing for the precise insertion of an endotracheal cannula.  
37 This cannula was subsequently interfaced with the ventilator, and key parameters—  
38 including Crs and Rrs—were recorded and processed using the integrated FlexiWare  
39 software.

40

### 41 **Cell Culture and Drug Treatment**

42 Sourced from Jennio Biotech (Guangzhou, China) and the Typical Culture Collection  
43 Committee of the Chinese Academy of Sciences (Shanghai, China), respectively,  
44 BEAS-2B and A549 cell lines were used in this study. BEAS-2B cells were grown in  
45 DMEM (12800, Gibco, Carlsbad, USA), while A549 cells were cultured in RPMI-1640  
46 (31800, Gibco, Carlsbad, USA), both of which were supplemented with 10% FBS  
47 (Hyclone) and a standard antibiotic mixture (100 U/mL penicillin and 100 µg/mL

48 streptomycin). Incubation was carried out under standard conditions of 37°C and 5%  
49 CO<sub>2</sub>.

50 As for primary mouse alveolar type II (AT2) cells, the isolation and extraction of these  
51 primary cells were conducted by Zhejiang Meisen Cell Technology Co., Ltd.  
52 (Hangzhou, China). Briefly, the lung vasculature was perfused with sterile PBS via the  
53 right ventricle to clear residual blood cells. The lungs were then inflated with dispase,  
54 followed by low-melting-point agarose. The lung tissue was subsequently dissociated  
55 into a single-cell suspension through mechanical mincing and enzymatic digestion.  
56 Primary AT2 cells were purified using a negative selection strategy involving magnetic  
57 bead depletion of CD45<sup>+</sup> leukocytes and CD31<sup>+</sup> endothelial cells, followed by  
58 differential adherence to remove fibroblasts.

59 The purified primary AT2 cells were cultured in specialized Mouse Primary Alveolar  
60 Type II Epithelial Cell Medium (CTCC-A005-MIC-CM, Meisen Cell, Hangzhou,  
61 China). The medium was supplemented with 100 U/mL penicillin and 100 µg/mL  
62 streptomycin to prevent microbial contamination. Cells were maintained in a  
63 humidified atmosphere at 37°C with 5% CO<sub>2</sub>.

64 All cell lines tested negative for mycoplasma contamination. Cells were treated with 5,  
65 10, or 20 µM Pral for qRT-PCR and Western blot analyses. In specified conditions,  
66 cells were co-treated with 20 ng/mL FGF2 (HY-P70440, MedChemExpress, USA) and  
67 50 ng/mL FGF10 (HY-P7048, MedChemExpress, USA).

#### 68 **TEER Measurement**

69 For the in vitro assessment of alveolar barrier robustness, A549 cells were plated at an  
70 initial density of  $5 \times 10^3$  cells per well into 24-well Transwell inserts (0.4 µm pore  
71 size; BIOFIL, China). After the specified experimental interventions, we quantified the

72 TEER. These measurements were conducted using an RE1600 epithelial volt-ohm  
73 meter sourced from Beijing Jingong Hongtai (China).

74

#### 75 **Dual-Luciferase Reporter Assay**

76 To evaluate transcriptional activity, we employed a dual-luciferase reporter system  
77 where Firefly luciferase acted as the primary reporter and Renilla luciferase served as  
78 an internal control for data normalization. The CREB1 overexpression and OCLN  
79 promoter-Luciferase plasmids were custom-synthesized by Wuhan MiaoLingBio  
80 (Wuhan, China). The experimental procedure began with the transfection of the CREB1  
81 expression vector, followed by a medium refresh after 5 hours. Subsequently, the  
82 OCLN promoter-Luciferase and Renilla constructs were introduced into cells at a 10:1  
83 ratio, with a second medium replacement performed 5 hours later. Luminescence was  
84 quantified by first equilibrating the culture plates to room temperature (30 min). Using  
85 the Duo-Lite Luciferase Assay System (Vazyme Biotech, Nanjing, China), Firefly  
86 activity was measured after a 10-minute incubation with the detection reagent. This was  
87 followed by the addition of Stop & Lite reagent to measure Renilla activity (10-minute  
88 incubation). Transcriptional potential was determined by calculating the Firefly/Renilla  
89 activity ratio.

#### 90 **Proteomics**

91 Proteomic profiling was conducted by Shanghai OE Biotech Co., Ltd. (Shanghai,  
92 China). Samples were analyzed using a Thermo Scientific Vanquish Neo UHPLC  
93 system coupled to an Orbitrap Astral mass spectrometer equipped with an Easy-spray  
94 ion source. The study design included a negative control (NC) group and an *FGFR1*-  
95 silenced (*siFGFR1*) group. Key procedural steps encompassed: protein extraction,

96 SDS-polyacrylamide gel electrophoresis (SDS-PAGE), in-solution digestion, liquid  
97 chromatography-tandem mass spectrometry (LC-MS/MS), and database searching.

### 98 **Transmission electron microscopy analysis**

99 For the assessment of pulmonary ultrastructure, lung specimens were obtained from the  
100 experimental mice and subjected to initial fixation in 1 mL of fresh 2.5% glutaraldehyde  
101 (PH9003, Scientific Phygene) for 2 hours at ambient temperature, prior to 4°C  
102 refrigeration overnight. Tissues then underwent a 1-hour secondary fixation in 1%  
103 osmium tetroxide, which was succeeded by a 30-minute en bloc staining process with  
104 2% uranyl acetate. Subsequent to graded dehydration and embedding in epoxy resin, a  
105 diamond knife was utilized to prepare ultrathin sections. Final visualization and  
106 morphological image acquisition were achieved using a TECNAI 10 transmission  
107 electron microscope (Thermo Fisher Scientific).

### 108 **Immunofluorescence Assay**

109 Following treatment, cultured cells in 96-well plates underwent two PBS washes,  
110 followed by fixation with 4% paraformaldehyde (P6148, Sigma-Aldrich, USA) for 20  
111 minutes and permeabilization with 0.1% Triton X-100 in PBS for 10 minutes at 4°C.  
112 Subsequent blocking utilized 4% bovine serum albumin (B2064, Sigma-Aldrich, USA)  
113 in PBS at 37°C for 30 minutes, after which primary antibody incubation proceeded  
114 overnight at 4°C. Following additional PBS washes, cells were exposed to Alexa Fluor  
115 594-conjugated secondary antibodies (A21206; 1:250, Thermo Fisher Scientific, USA)  
116 for 1 hour at room temperature. Nuclear counterstaining was performed using DAPI  
117 (D212, Dojindo, Japan) for 5 minutes, with fluorescence imaging conducted on a Leica  
118 TCS SP8 microscope.

### 119 **Western Blot**

120 Protein lysates were prepared from cellular samples using a lysis buffer formulation  
121 containing 150 mM NaCl, 50 mM Tris-HCl, 2 mM EGTA, 2 mM EDTA, 25 mM  $\beta$ -  
122 glycerophosphate, 25 mM NaF, 0.3% Triton X-100, 0.3% NP-40, 0.3% leupeptin, 0.1%  
123  $\text{NaVO}_3$ , and 0.1% PMSF. Aliquots of 30-50  $\mu\text{g}$  protein were electrophoretically  
124 resolved on 8%, 10%, or 12% SDS-polyacrylamide gels and transferred to 0.45  $\mu\text{m}$   
125 PVDF membranes (IPVH00010, Millipore). Membranes were blocked with non-fat  
126 milk prior to sequential incubation with primary and secondary antibodies, with protein  
127 detection achieved via ECL Plus chemiluminescent substrate (P2300, NCM Biotech).  
128 Primary immunoreagents included: FGFR1 (ET1612-62, HuaBio, China), CREB1  
129 (ET1601-15, HuaBio, China), OCLN (91131, CST, USA), ZO-1 (HA722797, HuaBio,  
130 China), Claudin-1 (HA721248, HuaBio, China), GAPDH (HA721136, HuaBio, China)

### 131 **Quantitative real-time PCR (qPCR)**

132 Following specified treatments, cellular and murine tissue samples underwent RNA  
133 extraction using TRIzol reagent (15596026, Thermo Scientific, USA). Equivalent RNA  
134 quantities were reverse transcribed into cDNA with a cDNA synthesis kit (AT311,  
135 TransGen Biotech, China). Quantitative real-time PCR amplification was conducted  
136 using TB Green Premix Ex Taq (Tli RNaseH Plus, RR420A, Takara, Japan) on a  
137 QuantStudio 3 system (A28132, Applied Biosystems, Singapore). Gene expression fold  
138 changes were derived via the  $2^{-\Delta\Delta\text{Ct}}$  method through comparative analysis of threshold  
139 cycle (Ct) values. Dual biological replicates were analyzed in technical duplicates, with  
140 expression data normalized to reference genes. Primer sequences were as follows:

141 *OCLN* forward: GCAAAGTGAATGACAAGCGG

142 *OCN* reverse: CACAGGCGAAGTTAATGGAAG  
143 *FGFR1* forward: AACCTGCCTTATGTCCAGATC  
144 *FGFR1* reverse: AGAGTCCGATAGAGTTACCCG  
145 *RET* forward: GGAGAAGGCGAATTTGGAAAAG  
146 *RET* reverse: CAGGACGTTGAACTCTGACAG  
147 *Ocln* forward: ACTATGCGGAAAGAGTTGACAG  
148 *Ocln* reverse: GTCATCCACACTCAAGGTCAG  
149 *Fgfr1* forward: AACTTGCCGTATGTCCAGATC  
150 *Fgfr1* reverse: AGAGTCCGATAGAGTTACCCG  
151 *GAPDH* forward: ACATCGCTCAGACACCATG  
152 *GAPDH* reverse: TGTAGTTGAGGTCAATGAAGGG  
153 *Gapdh* forward: CTTTGTCAAGCTCATTTCCTGG  
154 *Gapdh* reverse: TCTTGCTCAGTGTCTTGC

155

## 156 **Cell transfection**

157 BEAS-2B and A549 cells were plated in 12-well plates at  $5 \times 10^4$  cells/well and cultured  
158 until reaching ~50% confluence. Transfection was performed using Polyplus  
159 Transfection reagent (409-10, France) with either non-targeting control siRNA or gene-  
160 specific siRNA oligonucleotides per manufacturer's protocol. Gene-specific siRNA  
161 sequences were provided by GenePharma (China) as follows:

162

163 si *CEBPB* sense: 5'- CCUCGCAGGUCAAGAGCAA(dT)(dT)-3'

164 si *CREB1#1* sense: 5'- CCAACAAAUGACAGUUCAA(dT)(dT)-3'

165 si *DDX5* sence: 5'- GCUUCGUGAAGCUAAUCAAA(dT)(dT)-3'  
166 si *RUNX1* sence: 5'- CUCAAUCGGCUUGUUGUGA(dT)(dT) -3'  
167 si *ZEB1* sence: 5'- CCUCUCUGAAAGAACACAUAUA(dT)(dT) -3'  
168 si *ELF1* sence: 5'- CAAGGCUACUUGUCCUAAA(dT)(dT) -3'  
169 si *SUZ12* sence: 5'- CAAUACAAGGCAACAAACU(dT)(dT)-3'  
170 si *TAF7* sence: 5'- GGUAUUCGGUCACAGCAUA(dT)(dT)-3'  
171 si *KLF4* sence: 5'- GCAGCUUCACCUAUCCGAU(dT)(dT)-3'  
172 si *YY1* sence: 5'- CGACGACUACAUGAACAA(dT)(dT)-3'  
173 si *TCF12* sence: 5'- CAUUCAGUCCUGUCUAGUA(dT)(dT) -3'  
174 si *CREB1#2* sence: 5'- GCAGCUCAUGCAACAUCAU(dT)(dT)-3'  
175 si *FGFR1#2* sence: 5'- CUAUCGGACUCUCCCAUCA(dT)(dT)-3'  
176 si *DDR1* sence: 5'- CCCUCUGCAUGAUUACUGA(dT)(dT)-3'  
177 si *FLT3* sence: 5'- GGUGUCGAGCAGUACUCUA(dT)(dT)-3'  
178 si *JAK1* sence: 5'- GCGAUUAUUAUCCAGAAACA(dT)(dT)-3'  
179 si *JAK2* sence: 5'- CCAUCAUACGAGAUCUAAA(dT)(dT)-3'  
180 si *PDGFRB* sence: 5'- UUGAUCUGUAGCUGGAAGG(dT)(dT)-3'  
181 si *FGFR1#1* sence: 5'- CUAUCGGACUCUCCCAUCA(dT)(dT)-3'  
182 si *FGFR2* sence: 5'- CCACGGACAAAGAGAUUGA(dT)(dT)-3'  
183 si *NTRK1* sence: 5'- GGAAGUUCAUCCAGUGUUA(dT)(dT)-3'  
184 si *NTRK3* sence: 5'- CGAUGGUUUCAGACGCUGAAG-3'  
185 si *VEGFR2* sence: 5'- GGAAGAUAGUGAAAUAACA (dT)(dT)-3'

186

187 **Statistical Analysis**

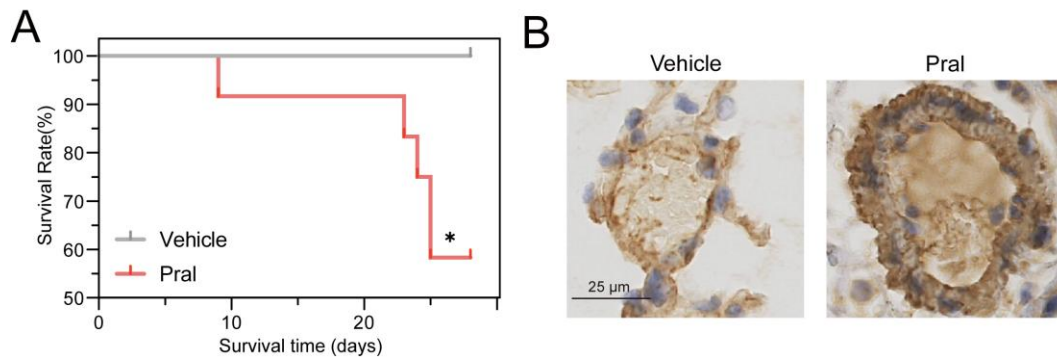
188 Statistical analyses were executed with GraphPad Prism 8.0. Results are expressed as  
189 mean  $\pm$  SEM. Intergroup comparisons employed unpaired two-tailed Student's t-tests,  
190 while multigroup analyses utilized one-way ANOVA.

191

192 **Funding:** This study was supported by the Central Guidance for Local Science and  
193 Technology Development Fund Project (No. 2024ZY01047 to Dr. Luo) and the  
194 National Natural Science Foundation of China (No. 82173893 to Dr. Luo).

195

196



198

199 **Figure S1. Pral-associated fatal interstitial lung disease.**

200 (A) Survival curve of Vehicle- and Pral-treated (100 mg/kg/d) mice over 4 weeks. (B)

201 Representative IHC images demonstrating pulmonary vascular remodeling in lung

202 tissues from Vehicle- and Pral-treated mice. Statistical significance for survival was

203 determined using the Log-rank (Mantel-Cox) test. Significance thresholds: \* ( $P < 0.05$ ).

204

205

206

207

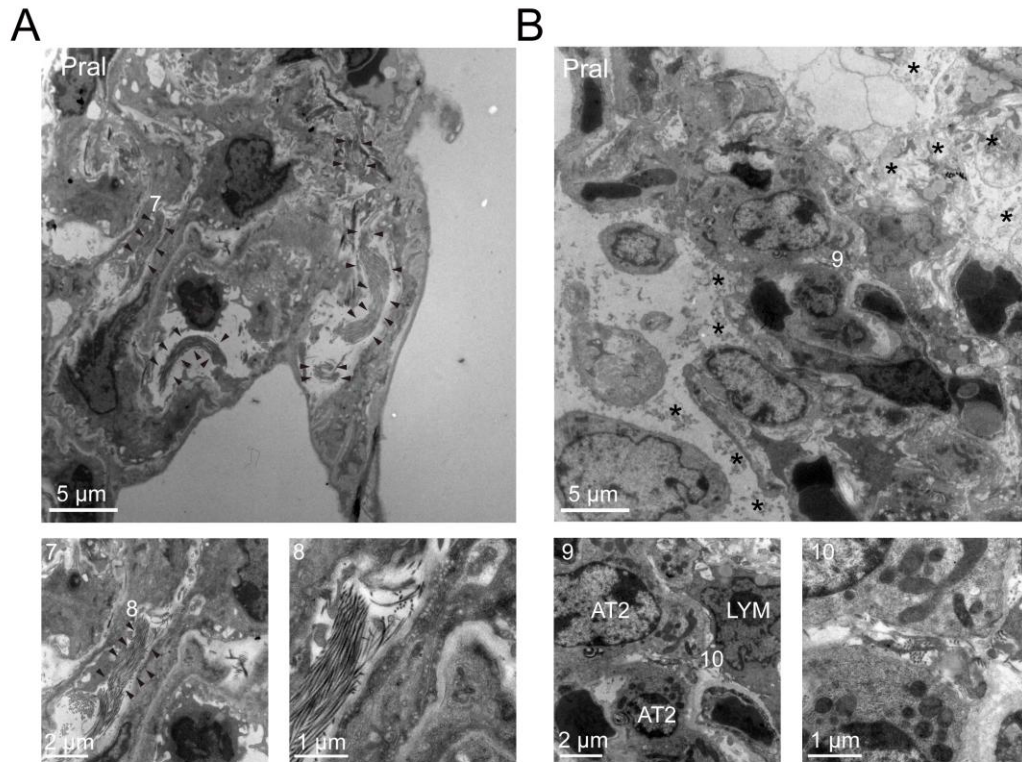
208

209

210

211

212



213

214 **Figure S2. Electron microscopy of Pral-triggered ultrastructural changes in the**  
 215 **Disrupted pulmonary epithelial TJ.**

216 (A-B) Damaged pulmonary epithelial cells after Pral treatment. (A: 7-8, Fibrotic  
 217 deposition, B: 9-10, Inflammatory cell infiltration ) AT1: Type I alveolar epithelial cell,  
 218 AT2: Type II alveolar epithelial cell, LYM: lymphocyte. Black arrows indicate fibrosis,  
 219 asterisks indicate evident parenchymal edema.

220

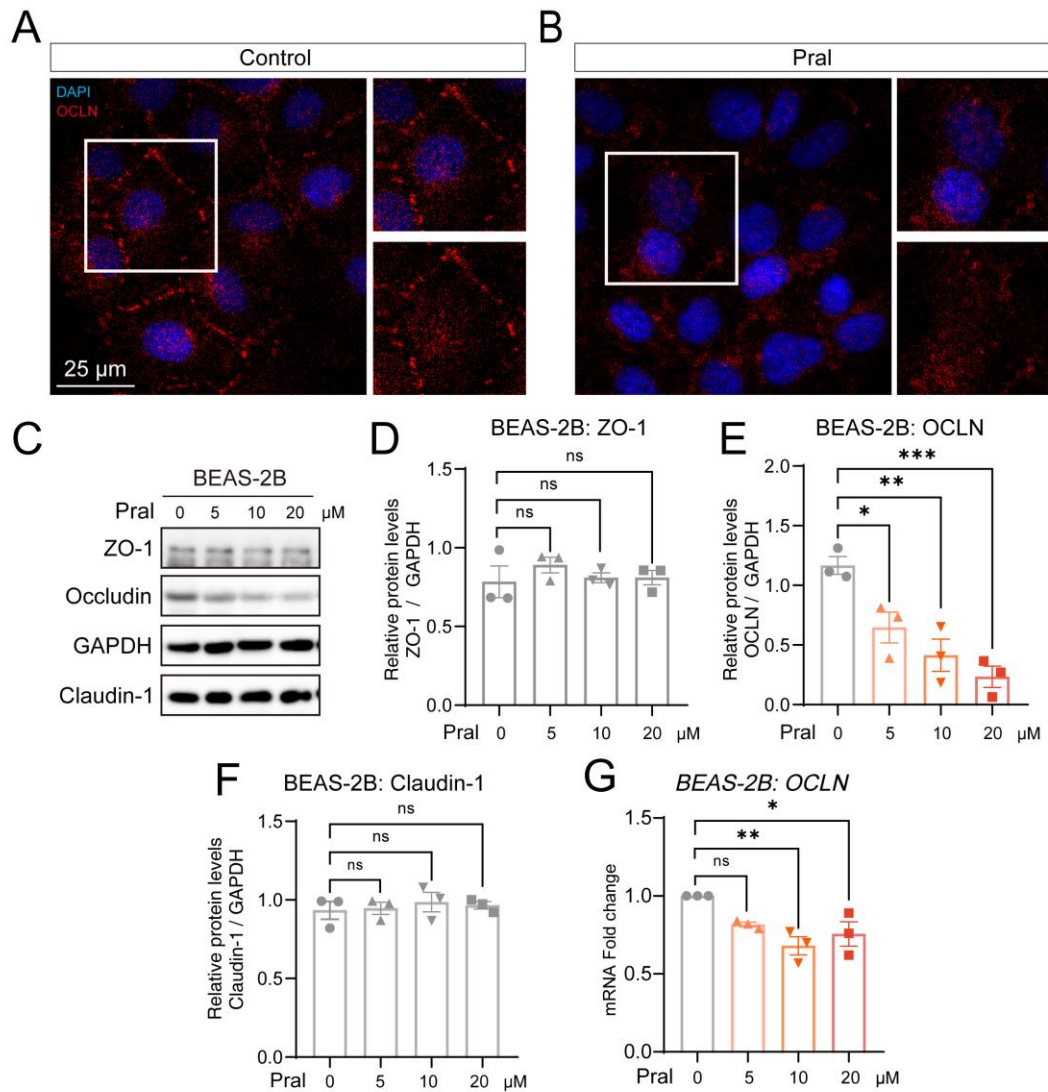
221

222

223

224

225



226

227 **Figure S3. Pral disrupts pulmonary epithelium TJ by suppressing OCLN**  
 228 **expression.**

229 (A-B) Immunofluorescence (IF) staining of OCLN (red) in pulmonary epithelial cells

230 BEAS-2B. (A) Control group. (B) Pral-treated group. (C-F) Western blot analysis of TJ

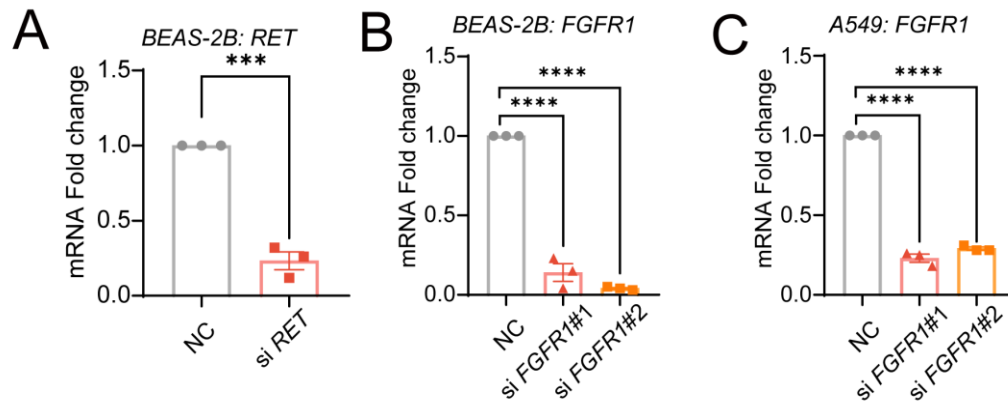
231 proteins in BEAS-2B cells. (C) Representative blots of ZO-1, OCLN, and Claudin-1.

232 (D-F) Quantification of protein levels for ZO-1 (D), OCLN (E), and Claudin-1 (F). (G)

233 qRT-PCR analysis of OCLN mRNA expression in BEAS-2B cells post-Pral treatment.

234 Statistical comparisons between multigroup analyses employed one-way ANOVA.

235 Significance thresholds: ns (not significant), \* ( $P < 0.05$ ), \*\* ( $P < 0.01$ ), \*\*\* ( $P < 0.001$ ).



236

237 **Figure S4. Pral reduces OCLN expression through FGFR1 inhibition.**

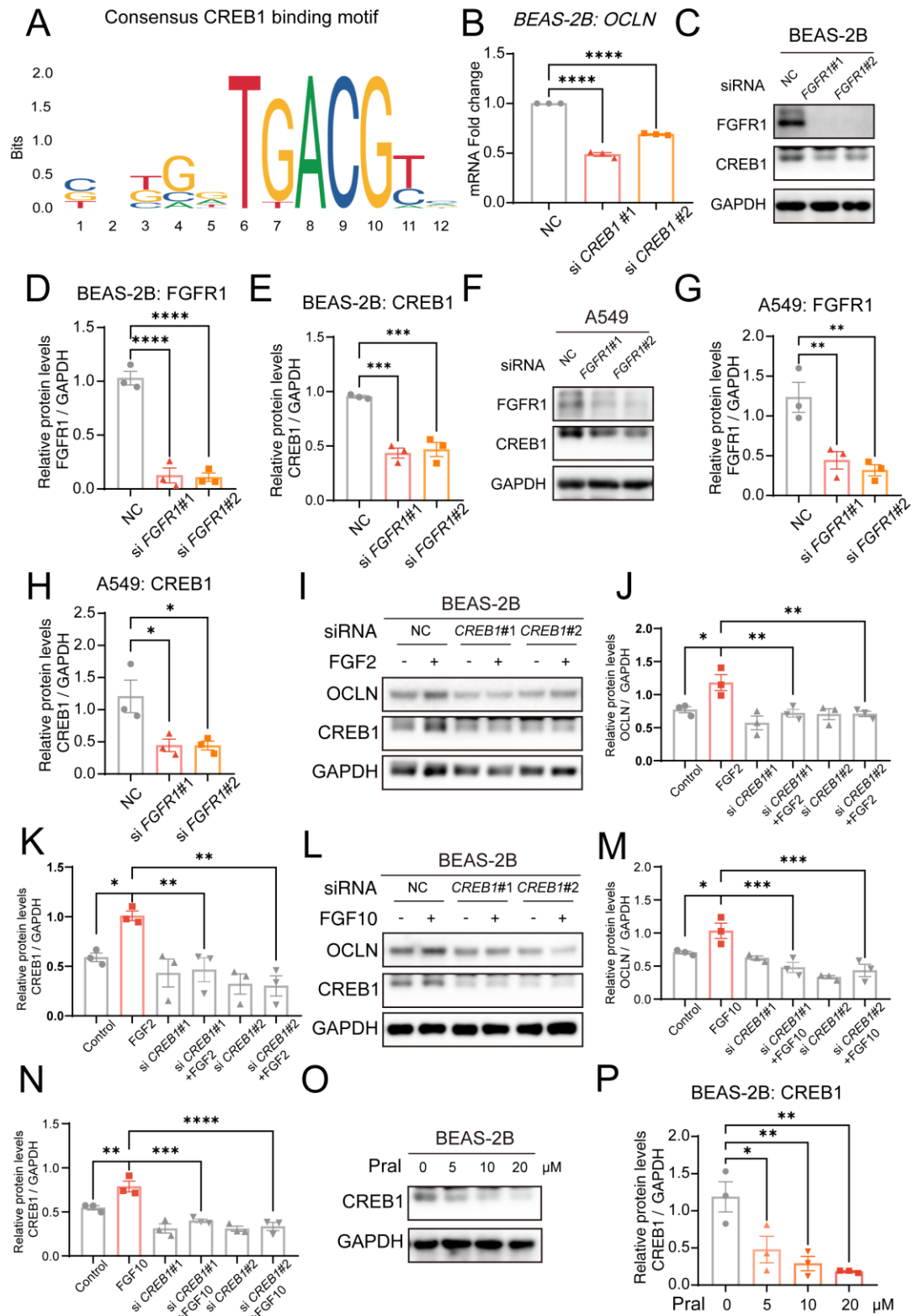
238 (A) RET knockdown efficiency in BEAS-2B cells transfected with siRET . (B) *FGFR1*

239 knockdown efficiency in BEAS-2B cells transfected with si*FGFR1*. (C) *FGFR1*

240 knockdown efficiency in A549 cells transfected with si*FGFR1*.

241

242



243

244 **Figure S5. FGFR1 inhibition reduces OCLN transcription via CREB1 suppression.**

245 (A) Schematic of CREB1 binding sites on OCLN promoter predicted by JASPAR

246 database. (B) qRT-PCR analysis of OCLN mRNA in CREB1-silenced BEAS-2B cells.

247 (C-E) Western blot analysis in *FGFR1*-silenced BEAS-2B cells. (C) Representative  
248 blots of FGFR1 and CREB1. (D) Quantification of FGFR1.(E) Quantification of  
249 CREB1. (F-H) Western blot analysis in *FGFR1*-silenced A549 cells. (F) Representative  
250 blots. (G) Quantification of FGFR1. (H) Quantification of CREB1. (I-K) Western blot  
251 analysis in BEAS-2B cells stimulated with FGF2 (+/- si-*CREB1*). (I) Representative  
252 blots; (J-K) Quantification of OCLN and CREB1 levels. (L-N) Western blot analysis in  
253 BEAS-2B cells stimulated with FGF10 (+/- si-*CREB1*). (L) Representative blots; (M-  
254 N) Quantification of OCLN and CREB1 levels. (O-P) Western blot analysis and  
255 quantification of CREB1 expression in Pral-treated BEAS-2B cells.

256

257

258

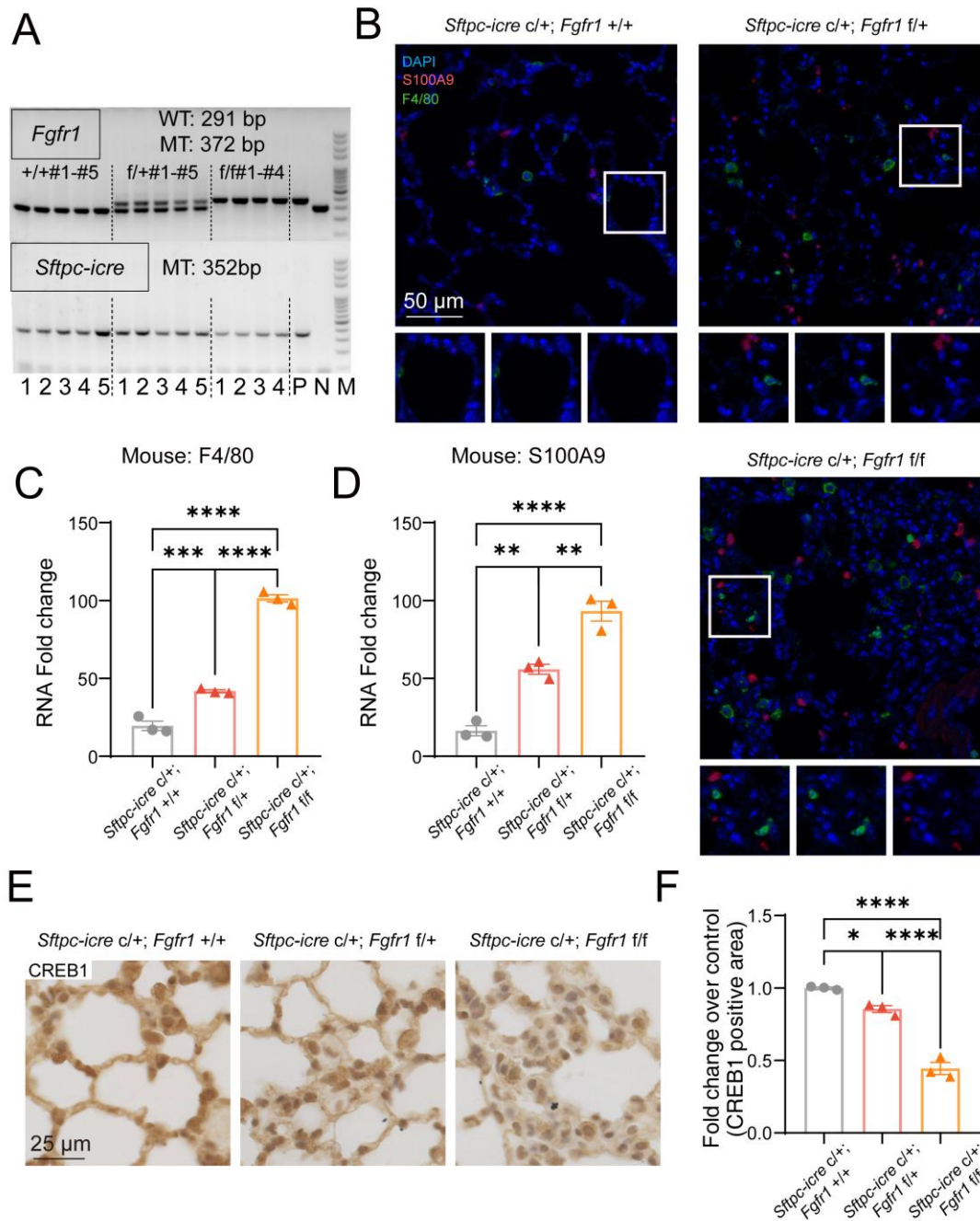
259

260

261

262

263



264

265 **Figure S6. Lung Epithelial-Specific *Fgfr1* Knockout Induces Inflammatory**

266 **Infiltration and Reduces CREB1 Expression.** (A) Genotyping results confirming

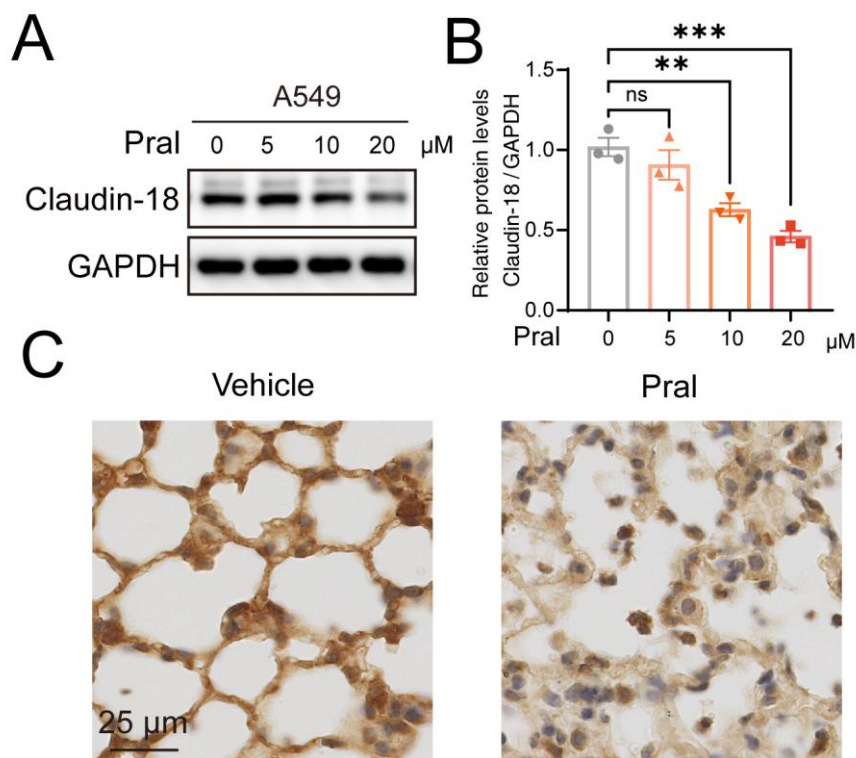
267 lung epithelial-specific *Fgfr1* knockdown/knockout (KD/KO) in mice. (B-

268 D) Multiplex immunohistochemistry (mIHC) and quantification of immune cell

269 infiltration in lung tissues from control and *Fgfr1* KD/KO mice. (B) Representative

270 mIHC images of F4/80<sup>+</sup> macrophages (green) and S100A9<sup>+</sup> neutrophils (red). (C-

271 D) Quantification of average fluorescence intensity for F4/80 (C) and S100A9 (D). (E-  
 272 F) IHC and quantification of CREB1 expression in lung tissues. (E) Representative IHC  
 273 images of CREB1 in control and *Fgfr1* KD/KO mice. (F) Quantification of CREB1  
 274 IHC-positive area. Statistical comparisons between multigroup analyses employed one-  
 275 way ANOVA. Significance thresholds: ns (not significant), \* ( $P < 0.05$ ), \*\* ( $P < 0.01$ ),  
 276 \*\*\* ( $P < 0.001$ ), \*\*\*\* ( $P < 0.0001$ ).



277 Figure S7: Pralsetinib suppresses Claudin-18 expression in lung epithelium and tissues.  
 278 (A-B) Western blot analysis of Claudin-18 expression in A549 cells following Pral  
 279 treatment. (A) Representative protein bands for Claudin-18 and GAPDH; (B)  
 280 Quantitative analysis of Claudin-18 protein levels normalized to GAPDH. (C)  
 281 Representative immunohistochemistry (IHC) images demonstrating the expression and  
 282 distribution of Claudin-18 in mouse lung tissues from the Vehicle and Pral-treated

283 groups. Data are presented as mean  $\pm$  SEM from at least three independent biological  
284 replicates. Statistical significance was determined using one-way ANOVA. ns (not  
285 significant), \*\*:  $P < 0.01$ ; \*\*\*:  $P < 0.001$ .